



MODELING OF ELASTIC ANISOTROPY DUE TO ONE-DIMENSIONAL PLASTIC CONSOLIDATION OF CLAYS

T. HUECKEL and E. TUTUMLUER

Department of Civil Engineering, Duke University, Durham, NC 27706

ABSTRACT

Experiments indicate that in one-dimensionally consolidated natural clays the elastic anisotropy is much stronger than the plastic strain anisotropy. Moreover, the elastic anisotropy appears to be dependent on the pre-consolidation strain. Coupled elasto-plastic constitutive law is shown to be able to simulate these anisotropy effects of natural clay deposits. In this law the elastic potential is not only a function of stress, but additionally of the plastic strain. The plastic strain comprises the geological process of pre-consolidation idealized as an one-dimensional plastic straining as well as a mechanically induced strain due to engineering activity. Calibration of the model and simulation of some stress paths are presented and related to the classical experimental results by Mitchell (1972).

INTRODUCTION

Natural clays are often anisotropic because their past sedimentation and consolidation processes were both driven by the gravity. Both elastic and plastic behavior may be anisotropic. The simplest way to detect this sort of anisotropy is to perform an isotropic compression test. In such a test, all stress components are equal. However, in response to this load, materials which are anisotropic develop unequal strain components. In this way,

Mitchell (1972) found that a one-dimensionally lightly overconsolidated kaolin exhibits only elastic anisotropy, while plastic strains are almost isotropic during isotropic compression. Mitchell has also seen that in an isotropic unloading, the elastic strain was almost entirely uniaxial. On the other hand, in undrained triaxial compression at various isotropic pressures, the effective stress paths revealed an anisotropy, and in particular were found sensitive to the demise of the anisotropy induced by a subsequent isotropic loading, Mitchell (1972).

Graham et al. (1983), and Wood and Graham (1989) investigated a large number of clays and concluded that the elastic domain in overconsolidated clays has an elliptic shape in p' , q plane, however the ellipse is centered on the K_0 - line, rather than on isotropic stress axis, Figure (1). They also found that elastic behavior is anisotropic and may be described by a hypoelastic, transversely isotropic model proposed earlier by Graham and Houlby (1983). Subsequently Wood and Graham (1989) proposed a generalized version of Cam-clay model to describe the above form of anisotropy. However, they limit the validity of their model to small variations of stress around the rotated yield surface, without allowing for further changes in the rotation. A rotated yield surface was also detected experimentally for other one-dimensionally consolidated materials by Parry and Nadarajah (1974); Drescher, Hueckel, and Mroz (1974); Tavenas and Leroueil (1977); Ko and Sture (1980); Jamiolkowski et al. (1985).

Classically, induced anisotropy is distinguished from inherent anisotropy. The latter one is usually related to fabric orientation and is believed to be a material property. The former one is considered as being produced during an irreversible deformation process and thus is dependent on the material history, (see e.g., Lewin, 1973; Anandarajah and Dafalias, 1986). Most of elastoplastic models which address jointly both induced and inherent anisotropy are based on rotational hardening plasticity, Hashiguchi (1979), Ghaboussi and Momen (1982), Kavvadas (1983), Banerjee et al. (1984), Anandarajah and Dafalias (1986). However, they consider plastic anisotropy only.

This paper focuses on the elastic anisotropy of one-dimensionally preconsolidated clays. It is assumed that the elastic anisotropy results from anisotropy of plastic strain during the one-dimensional preconsolidation. This means that geological history of consolidation of soil is simulated as a one-dimensional plastic strain process. The elastic behavior is then assumed as dependent on the amount of the plastic strain accumulated in such a process. This is described by means of elastoplastic coupling (see Hueckel, 1975, 1976, 1985; Maier and Hueckel, 1979; Dafalias, 1977).

Plasticity is described by a Cam-clay like theory, with a rotating, as well as isotropically expanding yield surface. The model is calibrated on some part of experiments of Mitchell (1972), while another part of his experiments serves as a basis for comparison with the model predictions. Mitchell's experiments are particularly attractive, because in his tests the clay remains transversely isotropic. Moreover, in both one-dimensional strain and isotropic loading, principal stress and principal strain values were measured. The considered dependence on pre-consolidation strain is of particular practical importance, when clay strata with different overconsolidation ratios are to be considered.

ONE-DIMENSIONAL PLASTIC CONSOLIDATION

In what follows the whole complex geological history of a clay soil mass will be substituted by one single process of consolidation and subsequent rebound due to exhumation caused by erosion. This means that the prior sedimentation process as well as possible subsequent tectonic processes are disregarded. Moreover, the following simplifying assumptions are made to make this consolidation mathematically tractable. First, we note that in the experiments with consolidation of clays from a slurry the reversible axial strains are much smaller than the corresponding irreversible strains, e.g. Burland (1967). Thus, reversible strain will be neglected in the pre-consolidation phase. Second, it is assumed that the consolidation is perfectly vertical, and thus one-

dimensional. This means that the horizontal component of strain is equal to zero, $\epsilon_{22} = 0$. It does not automatically imply that both elastic and plastic lateral strain components are zero, since the components may compensate each other. It is very difficult to evaluate the lateral elastic component in the actual naturally consolidated soil mass. But, it is known, for instance, that the lateral swell of deep excavations is much smaller than the vertical heave (see e.g. Moorhouse, 1972). However, from the form of, say linear-elastic stress potential, it results that the lateral elastic strain along a K_0 - stress path during 1-D consolidation is much smaller than the axial elastic strain. The above considerations seem to furnish a sufficient basis for the assumption that during the one-dimensional consolidation the axial plastic strain is a dominant strain component. Consequently, it will be assumed that the plastic axial strain is the only cause of change in elastic behavior during the consolidation period.

A constitutive model proposed, capable of taking into account the initial elastic anisotropy and the subsequent evolution of the induced elastic and plastic anisotropy, includes an elastoplastic coupling. According to this concept, elastic properties are affected by plastic strains. For overconsolidated natural clay deposits, elastic potential is thus dependent on the past preconsolidation strain, while with an increase in stress, exceeding the preconsolidation stress, the potential may further change as additional plastic strains start to accumulate.

Elastoplastic coupling as introduced by Hueckel (1975, 1976, and 1985), Maier and Hueckel (1977, 1979), and Dafalias (1977, 1979) consists in the fact that elastic properties of a solid depend on an additional variable, referred to as plastic prestrain μ_{ij} . For the present purposes plastic prestrain is defined as a sum of irreversible preconsolidation strain μ_{ij}^0 and current plastic strain ϵ_{ij}^p , which includes the

irreversible strain generated by mechanical departures from the in situ stress state. Hence,

$$\mu_{ij} = \mu_{ij}^0 + \int_{t_0}^t \frac{\partial \epsilon_{ij}^p}{\partial t} dt \quad ; \quad \mu_{ij}^0 = \int_{-\infty}^{t_0} \frac{\partial \epsilon_{ij}^p}{\partial t} dt \quad (1)$$

where t_0 is the origin of the time scale of the application of mechanical (non-geological) loads.

It should therefore be clear that μ_{ij}^0 is a strain equivalent of a geological deformation process symbolically taken as occurring between $-\infty$ and time t_0 . Finally, we assume that this is a one-dimensional strain process and that it can be measured by the difference between the current and a presumed initial void ratio. The latter one can be obtained through an extrapolation of the one-dimensional K_0 compressive stress-void ratio relationship measurable in laboratory.

In the forthcoming sections, the elasticity law chosen, and the particular forms of its coupling to plastic prestrain, will be first explained. For a more complete presentation of the concept of elastoplastic coupling, see Hueckel, (1975, 1976), Maier and Hueckel, (1979). Plastic anisotropic hardening is then described for triaxial conditions. Its general presentation is given in Appendix I.

ELASTICITY

The elastoplastic coupling is proposed to be in the anisotropic form, so that the elastic energy depends on a directional (tensor) variable μ_{ij} . The elastic complementary energy function $V(\sigma'_{ij}, \mu_{ij})$ for clays is postulated to be in the following form

$$V = \frac{\kappa}{1 + e_0} p'_0 \left[\frac{p'}{p'_0} (\ln(p'/p'_0) - 1) + 1 \right] + \frac{1}{4G} (s_{ij} - s_{ij}^0) (s_{ij} - s_{ij}^0) + \text{coupling terms} \quad (2)$$

where the stress deviator and effective mean normal stress are defined as

$$s_{ij} = \sigma'_{ij} - p' \delta_{ij}; \quad p' = \frac{1}{3} \sigma_{kk}$$

and p'_0 and s_{ij}^0 in equation (2) are in situ isotropic effective stress and deviatoric stress tensor respectively and δ_{ij} is Kronecker symbol. The first two terms in (2) lead to the usual elastic law for soils, which is logarithmic in the isotropic and linear in the deviatoric part, respectively. Positive stress is compressive.

Two forms of the coupling term in the elastic complementary energy equation (2) are proposed: i) linear coupling, ii) logarithmic coupling. The corresponding expressions for the coupling part of the complementary elastic energy are thus as follows:

i) linear coupling:

$$\text{Coupling term} = \frac{1}{2} C_p M_1^2 \quad (3)$$

where

$$M_1 = \mu_{ij} (\sigma'_{ij} - \sigma_{ij}^0)$$

ii) logarithmic coupling:

$$\text{Coupling term} = C_{pl} M_0 \left[\frac{M_1}{M_0} \left(\ln \left(\frac{M_1}{M_0} \right) - 1 \right) + 1 \right] \quad (4)$$

where

$$\bar{M}_1 = \mu_{kl} \sigma'_{kl}$$

and

$$M_0 = \mu_{kl} \sigma_{kl}^0$$

In the above equations C_p and C_{pl} are preconsolidation constants, while M_1 and \bar{M}_1 are mixed invariants of stress and plastic prestrain differently defined for each case. M_0 is the reference value of the mixed invariant of in situ stress tensor σ_{kl}^0 and preconsolidation strain μ_{kl} .

If $\mu_{ij} = \mu_{ij}^0 + \varepsilon_{ij}^p$ with $\mu_{22} = \mu_{33} = 0$; $\mu_{11} \neq 0$ like in the case of one-dimensional consolidation, the mixed invariant M_1 takes on the form

$$M_1 = (\mu_{11}^0 + \varepsilon_{11}^p) \sigma'_{11} \quad (5)$$

With the above definitions of the coupling term, the elastic complementary energy (2) is always positive, see Hueckel, (1985). Thus, when the stress state is within a current yield surface, plastic deformation is constant and all strain is reversible upon the return to the initial stress. The elastic stress-strain law, by the usual potentiality rule reads:

i) in the case of linear coupling:

$$\varepsilon_{ij}^e = \frac{\partial V}{\partial \sigma'_{ij}} = \frac{1}{3} \frac{\kappa}{1 + e_0} \ln (P'/P'_0) \delta_{ij} + \frac{1}{2G} (s_{ij} - s_{ij}^0) + C_p M_1 \mu_{ij} \quad (6)$$

or, with the substitution of M_1

$$\varepsilon_{ij}^e = \frac{1}{3} \frac{\kappa}{1 + e_0} \ln (P'/P'_0) \delta_{ij} + \frac{1}{2G} (s_{ij} - s_{ij}^0) + C_p \mu_{ij} \mu_{kl} (\sigma'_{kl} - \sigma_{kl}^0) \quad (7)$$

ii) for logarithmic coupling:

$$\epsilon_{ij}^e = \frac{1}{3} \frac{K}{1 + e_0} \ln (P'/p'_0) \delta_{ij} + \frac{1}{2G} (s_{ij} - s_{ij}^0) + C_{pl} \ln \left(\frac{\mu_{kl} \sigma'_{kl}}{\mu_{kl} \sigma^0_{kl}} \right) \mu_{ij} \quad (8)$$

In the above equations, the first two terms are usual elastic terms for soils. The third term is the coupling term. It should be noted that from equations (6) and (8), it results that the principal directions of the elastic strain do not coincide with the principal directions of stress. In fact, a term μ_{ij} , having a constant direction within an immobile yield surface, is added to the usual elastic terms, to describe the permanent change in clay structure and thus in its elastic deformability. The mode of this strain is that of the summed up preconsolidation strain and newly produced plastic strain, through (1). Thus, it is seen from equation (7), that if the plastic strain is uniaxial, i.e., if μ^0_{11} is the only non-zero component of μ_{ij} , the elastic strain has a part, the direction of which does not depend on the current stress, but rather is that of the prestrain μ^0_{11} . This is exactly what was observed by Mitchell (1972). On the other hand, the intensity of this strain is proportional to stress projection on the plastic prestrain tensor. The closer the stress mode is to the prestrain mode, the greater is the influence of the prestrain on the elastic strain. Finally, when the stress returns to the original value, the elastic strain disappears according to its definition.

PLASTICITY

In this paper, the focus being on elastic anisotropy, the presentation of the plasticity model will be restricted to the axial symmetry stress case, such as occurs in triaxial

conditions (i.e. $\sigma'_1, \sigma'_2 = \sigma'_3$). The equations of a general model for anisotropic plastic behavior of clays in six dimensional stress space are given in Appendix I.

The proposed yield surface is assumed to have an elliptical shape as in the modified Cam-Clay model (Burland and Roscoe, 1969). However, in contrast to the Cam-Clay model, the yield surface here is assumed to undergo a combined growth and rotation, depending respectively on plastic volumetric strain and on plastic deviatoric strain and their history. Denoting by θ a generic angle of rotation in the p' - q plane, and by a the parameter governing the surface size, the equation of rotated yield function is as follows

$$f = \left[\frac{(p' + q \tan \theta)^2}{a / \cos \theta} \right] + \left[\frac{(-p' \tan \theta + q)^2}{N a / \cos \theta} \right] - 1 = 0 \quad (9)$$

where $p' = (\sigma'_1 + 2 \sigma'_3) / 3$, and $q = |\sigma'_1 - \sigma'_3|$, a is the major semi-axis and N (in principle a variable) is the ratio of the minor semi-axis b to the major semi-axis a . N at the state of uniaxial consolidation is obtained from the condition that the yield surface has a maximum at the critical state line $q / p' = M$. Such a yield surface rotated along the K_0 line is shown in Figure (2). This yield surface is assumed to account for the initial anisotropy developed during the one dimensional K_0 - consolidation. In p' - q plane, K_0 line is defined as

$$\tan \theta_0 = \left(\frac{q}{p'} \right)_0 = \frac{3(1 - K_0)}{1 + 2 K_0} \quad (10)$$

where θ_0 is the angle of inclination of K_0 - consolidation line measured from the isotropic axis.

A 3-dimensional representation of the yield surface in the principal stress space can be achieved considering an ellipsoid centered in the direction of an arbitrary straight radius passing through the origin of the p' - q - r stress space. Here r is defined as the third axis,

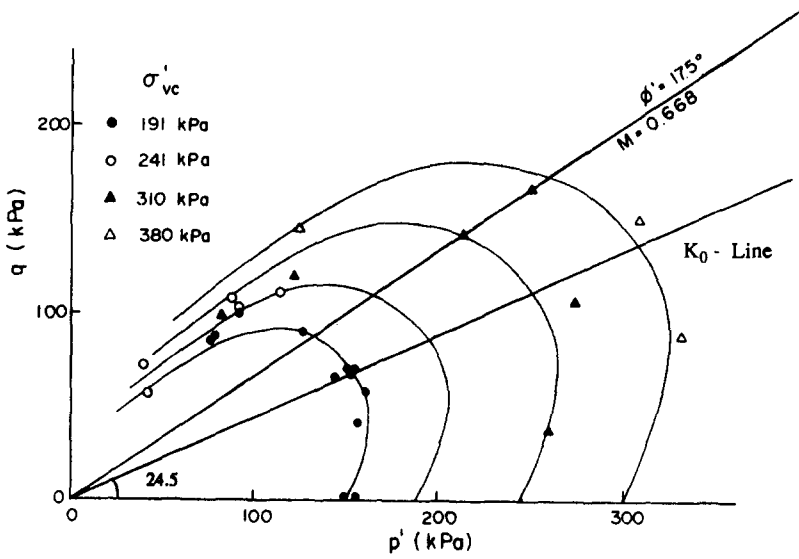


Figure 1: Yielding States of Overconsolidated Clay Samples In q - p' Plane (after Graham et al., 1983)

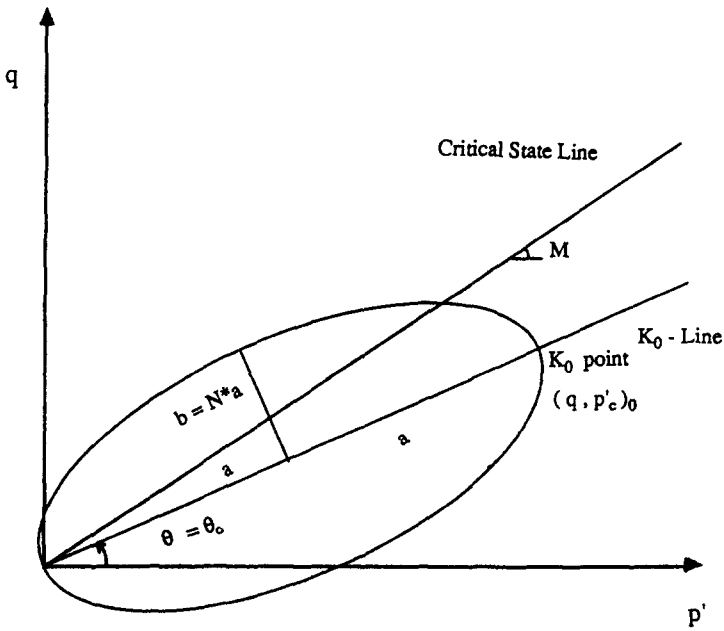


Figure 2: Rotated Yield Surface Due to One-Dimensional Consolidation

whose unit vector is perpendicular to p' - q plane in the principal stress space. In order to orient the apex of the ellipsoid along such a line, an additional angle of rotation α around q axis is introduced. The details of this configuration are given in Appendix I with the proper hardening equations defining the rotation angles in the general p' - q - r stress space.

To define the evolution of the yield surface, a combined isotropic-kinematic hardening law is adopted. The volumetric plastic strain rules the size of the surface, while the rotation is governed by the deviatoric plastic strain for the generation of anisotropy, and by the volumetric plastic strain for its demise. In order to characterize the current anisotropy two uncoupled hardening rules are proposed. The first one expresses the pattern of the growth of the yield locus dependent on the volumetric strain in the form

$$\bar{a} = a_0 \exp \left[\frac{(1 + e_0) \epsilon_v^p}{\lambda - \kappa} \right] ; \quad \bar{a} = a \cos \theta \quad (11)$$

where ϵ_v^p is the total accumulated volumetric plastic strain which includes the preconsolidation stage, a_0 is a reference pressure usually taken as unit value, and λ' and κ are constants. Note that this rule degenerates to the usual Cam-clay volumetric hardening law, if $\theta = 0$.

The hardening equation governing the rotation of the yield surface can be expressed through a non-dimensional rate evolution equation

$$d(\tan \theta) = \frac{q}{p'} [\delta \exp(-\delta \epsilon_q^p)] d\epsilon_q^p + D d\epsilon_v^p \quad (12)$$

where $\epsilon_q^p = \sqrt{\frac{2}{3}} \sqrt{e_{ij}^p e_{ij}^p}$ is the deviatoric plastic strain invariant, δ is a model parameter of the order of 10^2 and the function D corresponds to a plastic anisotropy demise mechanism discussed below. It is moreover assumed that at a hypothetical onset of

one-dimensional consolidation when $\varepsilon_q^p = 0$, also $\theta = 0$. Furthermore, it is assumed that $D = 0$ for $t < t_0$. Thus, when the uniaxial consolidation is advanced enough, the exponential part in (12) tends to zero, the rotation of the yield surface ceases and $\tan \theta$ tends to the current value of q/p' , in this case defined through equation (10). The latter one is ensured through the flow rule, as explained below.

A particular non-associated flow rule has been chosen to describe plastic strain behavior of lightly overconsolidated material like kaolin described by Mitchell (1972). This is not a universal type of plastic strain rate pattern for clays. Graham et al. (1983) observed a pattern that is much closer to an associated flow rule. Baldi et al. (1990) tested Boom clay which showed still another pattern. In an experiment of isotropic loading with a test program similar to that of Mitchell (1972), they found that the axial plastic strain component was dominant over the other two components. It must be emphasized that there is no single plastic strain rate flow rule for anisotropically consolidated clays and a non-associated flow rule offers a large flexibility to accommodate the behavior of various clays.

The flow rule is assumed as non-associated. This implies that there exists a plastic potential function $g = g(p', q)$ other than the yield function f , which defines the plastic strain rate as

$$d\varepsilon_{ij}^p = d\lambda \frac{\partial g}{\partial \sigma'_{ij}} \quad (13)$$

where $d\lambda$ is known as the plastic multiplier dependent on stress and plastic strain history.

The plastic potential incorporated in the model is assumed not to rotate as a result of the previous anisotropic stress history. It is taken to be composed of two, different size ellipses. The ratio between the two horizontal semi-axes is β and it is constant. Such a

potential has the functional form as introduced by Murff (1982).

$$g = \frac{1}{\beta^2} \left(\frac{p'}{a_p} - 1 \right)^2 + \left(\frac{q}{M a_p} \right)^2 - 1 = 0 \quad (14)$$

where a_p is the minor semi-axis of the plastic potential of the first ellipse and M is the slope of the critical state line (see Figure 3). Equation (14) is supplemented by the condition that $\beta = 1$ for $p' \leq a_p$. In this model constant β is defined through the hypothesis that the plastic strain rate at the maximum K_0 - consolidation state has only the vertical non-zero component, as discussed in the following section.

There are two essential features of the anisotropy development which we need to address through eq. (12). These are: formation of the inherent anisotropy during the uniaxial consolidation process and the evolution of the anisotropy (or induced anisotropy) during mechanical loading. In particular, the latter refers to anisotropy demise during isotropic loading. To deal with these two aspects of anisotropy evolution, the following assumptions are made. The shear induced plastic anisotropy is active all the time, including $t < t_0$, i.e., during initial one-dimensional preconsolidation and any mechanically induced plastic history. In addition, during mechanically induced processes, i.e., for $t \geq t_0$ there is an active mechanism of anisotropy demise induced by plastic compaction. This is described by the following rules complementing eq. (12):

$$\begin{aligned} t < t_0 : D &= 0 \\ t \geq t_0 \ \&\ (q/p') < (q/p')_0 : D = \gamma \left[\frac{q}{p'} - \tan\theta \right] \\ t \geq t_0 \ \&\ (q/p') \geq (q/p')_0 : D &= 0 \end{aligned} \quad (15)$$

where γ is a demise constant, while $(q/p')_0$ is the K_0 consolidation stress path, when $\tan\theta = q/p'$, $D = 0$. Moreover, during isotropic consolidation, as seen from eq. (12), only the demise part of the evolution is active, since $q = 0$. For instance, if the initial

position of the yield surface before the isotropic consolidation is at K_0 , with $\theta = \theta_{k0}$
 $= \tan^{-1}(q/p)_0$, then $\tan\theta$ can be integrated for the isotropic process to give

$$\frac{\tan \theta}{\tan \theta_{K_0}} = \exp [-\gamma (\Delta \epsilon_v^p)] \quad (16)$$

where $\Delta \epsilon_v^p$ refers to the plastic volumetric strain accumulated during the isotropic consolidation.

STRAIN-STRESS RELATIONSHIPS

In this section, total coupled elastoplastic rate stress-strain relationships will be derived. First, it should be noted that during the plastic process, an additional irreversible strain is generated due to elastoplastic coupling. This irreversible strain is the result of the irreversible variation of elastic properties with plastic strain, as may be seen in Hueckel (1975 and 1976). The total irreversible strain rate comprises, besides this strain rate, the plastic strain rate which may be unlimited, and proportional to stress rate as opposed to the former one which is proportional to the stress itself. Thus

$$d\epsilon_{ij}^{irr} = d\epsilon_{ij}^p + \frac{\partial^2 V}{\partial \sigma'_{ij} \partial \mu_{kl}} d\mu_{kl} = d\lambda \frac{\partial g}{\partial \sigma'_{ij}} + \frac{\partial^2 V}{\partial \sigma'_{ij} \partial \mu_{kl}} d\mu_{kl} \quad (17)$$

substituting from equations (7) or (8) the specific forms of the complementary energy V for linear and logarithmic coupling cases yield respectively

i) for linear coupling:

$$d\epsilon_{ij}^{irr} = d\lambda \frac{\partial g}{\partial \sigma'_{ij}} + C_p (\sigma'_{kl} - \sigma_{kl}^0) [\mu_{kl} d\mu_{ij} + \mu_{ij} d\mu_{kl}] \quad (18)$$

ii) for logarithmic coupling:

$$d\epsilon_{ij}^{irr} = d\lambda \frac{\partial g}{\partial \sigma'_{ij}} + C_{pl} \left[\ln \left(\frac{\mu_{kl} \sigma'_{kl}}{\mu_{kl} \sigma^0_{kl}} \right) d\mu_{ij} + \mu_{ij} \left(\frac{d\mu_{kl} \sigma'_{kl}}{\mu_{kl} \sigma'_{kl}} \right) \right] \quad (19)$$

Moreover, knowing that the plastic prestrain rate is described through (1) by the relationship

$$d\mu_{ij} = d\lambda \frac{\partial g}{\partial \sigma'_{ij}} \quad (20)$$

The total strain rate can be expressed for both cases as follows

i) linear coupling:

$$d\epsilon_{ij} = \left\{ \frac{1}{3} \frac{\kappa}{1 + e_0} \frac{dp'}{p'} \delta_{ij} + \frac{1}{2G} ds_{ij} + C_p \mu_{ij} \mu_{kl} d\sigma'_{kl} \right\} + d\lambda \left\{ C_p (\sigma'_{kl} - \sigma^0_{kl}) \left[\mu_{kl} \frac{\partial g}{\partial \sigma'_{ij}} + \mu_{ij} \frac{\partial g}{\partial \sigma'_{kl}} \right] + \frac{\partial g}{\partial \sigma'_{ij}} \right\} \quad (21)$$

ii) logarithmic coupling:

$$d\epsilon_{ij} = \left\{ \frac{1}{3} \frac{\kappa}{1 + e_0} \frac{dp'}{p'} \delta_{ij} + \frac{1}{2G} ds_{ij} + C_{pl} \mu_{ij} \frac{d\sigma'_{kl} \mu_{kl}}{\sigma'_{mn} \mu_{mn}} \right\} + d\lambda \left\{ C_{pl} \left[\ln \left(\frac{\mu_{kl} \sigma'_{kl}}{\mu_{mn} \sigma^0_{mn}} \right) \frac{\partial g}{\partial \sigma'_{ij}} + \mu_{ij} \frac{\sigma'_{rs}}{\mu_{mn} \sigma'_{mn}} \frac{\partial g}{\partial \sigma'_{rs}} \right] + \frac{\partial g}{\partial \sigma'_{ij}} \right\} \quad (22)$$

It is clear from the above equation that even if the plastic strain rate is normal to the plastic potential, the rate of irreversible strain is not. The irreversible strain rate always deviates from the normal by a vector colinear with the current plastic prestrain vector. The relative equations for the case of axial symmetry are presented in Appendix II.

Following the standard plasticity argument, the plastic multiplier $d\lambda$ is obtained from

the consistency condition which reads

$$df = \frac{\partial f}{\partial q} dq + \frac{\partial f}{\partial p'} dp' + \frac{\partial f}{\partial \epsilon_v^p} d\epsilon_v^p + \frac{\partial f}{\partial \epsilon_q^p} d\epsilon_q^p = 0 \quad (23)$$

where

$$\epsilon_q^p = \sqrt{\frac{2}{3}} \sqrt{e_{ij}^p e_{ij}^p} \quad \text{and} \quad e_{ij}^p = \epsilon_{ij}^p - \frac{1}{3} \epsilon_v^p \delta_{ij}$$

Since the yield function f is a function of both volumetric and deviatoric strains, through the hardening rule (12), equation (26) and flow rule (13) yield the multiplier $d\lambda$ in the form

$$d\lambda = \frac{1}{H} \left(\frac{\partial f}{\partial q} dq + \frac{\partial f}{\partial p'} dp' \right) \quad (24)$$

where H is the hardening modulus given by

$$H = - \left[\frac{\partial f}{\partial a} \left(\frac{\partial a}{\partial \bar{a}} \frac{\partial \bar{a}}{\partial \epsilon_v^p} + \frac{\partial a}{\partial \theta} \frac{\partial \theta}{\partial \epsilon_v^p} \right) \frac{\partial g}{\partial p'} + \frac{\partial f}{\partial \theta} \frac{\partial \theta}{\partial \epsilon_q^p} \frac{\partial \epsilon_q^p}{\partial e_{ij}^p} \frac{\partial g}{\partial s_{ij}} \right] \quad (25)$$

With the definition of the plastic multiplier, the governing equations of the elastoplastic coupling model have been established. The usual plastic loading and unloading criteria apply.

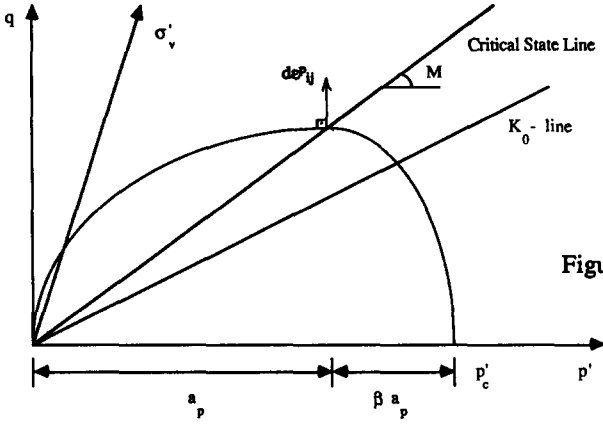
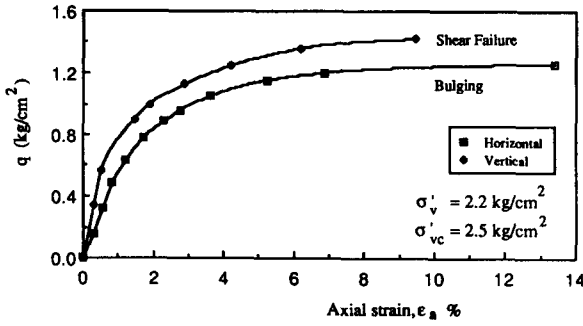
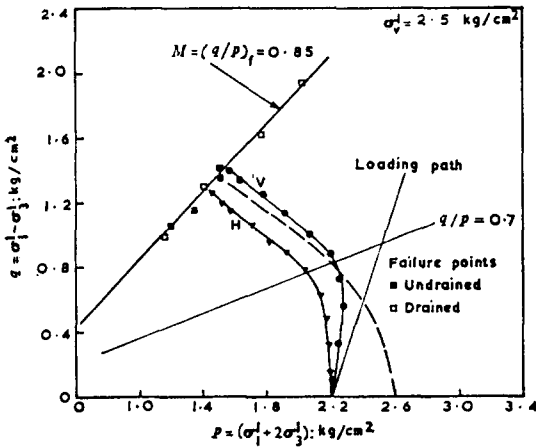


Figure 3: Plastic Potential



(a) Stress-Strain Curves



(b) Effective Stress Path

Figure 4: Undrained Triaxial Compression Test Results (after Mitchell, 1972)

IDENTIFICATION OF MODEL PARAMETERS

Data needed to identify the model parameters are obtained from a part of the experiments performed by Mitchell (1972). Mitchell has trimmed vertical and horizontal specimens from one-dimensionally consolidated blocks of kaolin. Maximum vertical pressure during consolidation was from a slurry at 160 % moisture content was $\sigma'_{vc} = 2.5 \text{ kg/cm}^2$. The blocks were then allowed to rebound to atmospheric pressure under small stress decrements and were stored for several days in a humid atmosphere in order to obtain zero stress condition. In such a process the material has acquired a transversal anisotropy.

The above described preparation technique simulates a uniaxial consolidation process of a naturally deposited clay in its geological past. Furthermore, the unloading of the specimens to atmospheric pressure at the end of the one-dimensional consolidation corresponds to a rebound due to the erosion of overburden.

The clay used for experiments was kaolin with liquid limit $LL = 74$, plasticity index $PI = 32$, activity coefficient = 0.44, and specific gravity, $G_s = 2.61$. Mitchell (1972) also performed a number of conventional undrained triaxial compression tests on vertically and horizontally trimmed specimens after initial isotropic reconsolidation to confining pressure, $\sigma'_0 = 2.2 \text{ kg/cm}^2$, i.e., less than the maximum vertical past pressure $\sigma'_{vc} = 2.5 \text{ kg/cm}^2$. The failure of all specimens was observed to occur close to a line where $M = (q / p')_f = 0.85$, corresponding to the internal friction angle $\phi' = 22$ degrees. Effective stress paths in undrained tests are shown in Figure (4). Also in this figure an undrained effective stress path is shown after an isotropic consolidation to 2.6 kg/cm^2 . This stress path was nearly identical for the vertically and horizontally trimmed specimens.

To study anisotropy in isotropic compression Mitchell performed a number of tests by applying cycles of isotropic pressure increments. The normalized strain increments plotted in Figure (5) show the development of axial and radial strains during the isotropic consolidation and unloading for both vertical and horizontal specimens. The strain rates are

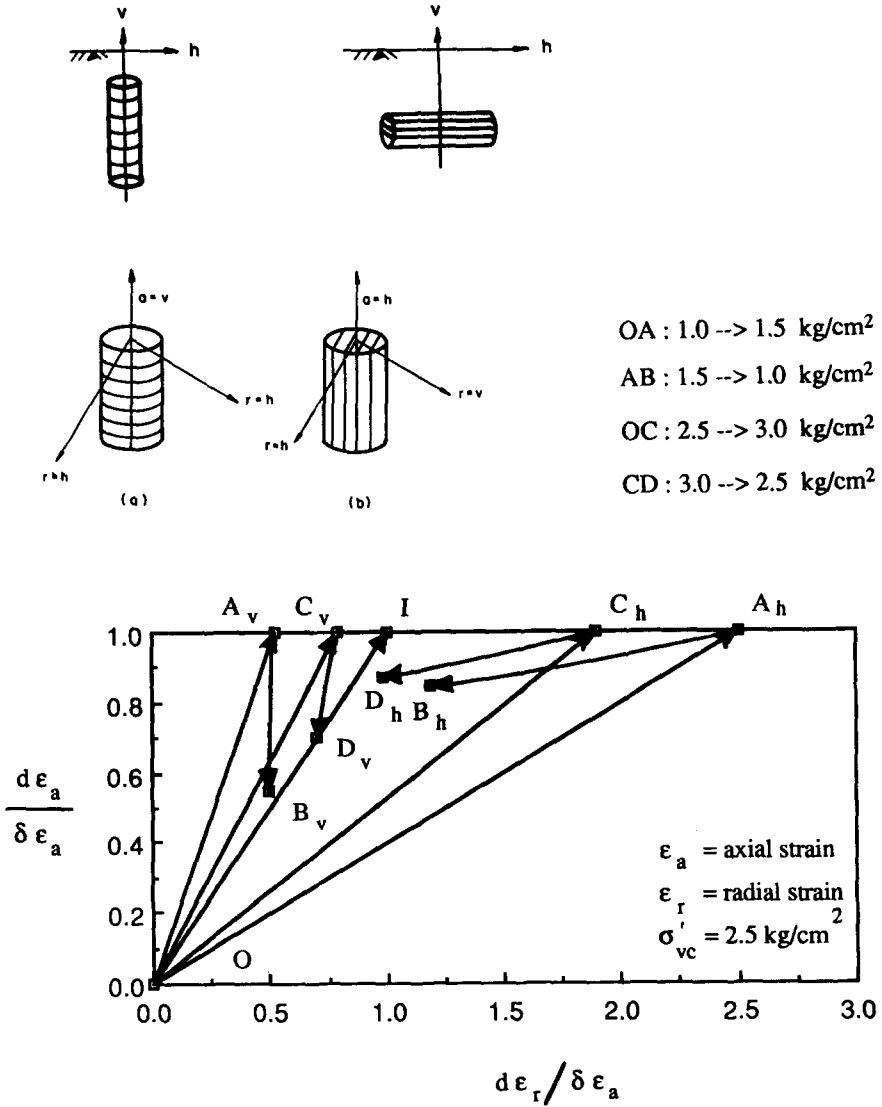


Figure 5: Strain Increment Response of Vertical and Horizontal Specimens to Isotropic Pressure Changes (Recalculated after Mitchell, 1972)

normalized with respect to the maximum incremental axial strain during the initial isotropic consolidation increment for each cycle plotted.

The vectors OA_v and A_vB_v represent the normalized strain increments developed in the vertical specimen during an effective pressure increase from 1.0 to 1.5 kg/cm² and a subsequent isotropic effective pressure decrease from 1.5 to 1.0 kg/cm² respectively. Note that for the same effective stress cycle on horizontal specimens, the vectors OA_h and A_hB_h are again normalized with respect to the maximum incremental axial strain, however this time, axial strain direction corresponds to the horizontal direction in the vertically consolidated mass. In fact, during the isotropic loading, the axial strain and one of the lateral (in situ-horizontal), strain components are equal, while the other lateral (in situ-vertical) strain is different (see the inset in Fig. 5). Furthermore, the values on the axis of radial strain in Figure (5) have been calculated by Mitchell from the volume changes with the assumption that the cross section of the specimen maintains its circular shape throughout the test. While this is an acceptable assumption for vertical specimens, it is not in principle for horizontal specimens during isotropic tests. To make the data consistent, the vectors OA_h and A_hB_h corresponding to the experimental results of the horizontal specimens (Mitchell,1972) are recalculated in Figure (5) under an alternative assumption that $\epsilon_{ah} = \epsilon_{rh}$. The data of Figure (5) are extended in Figure (6) to compare the volumetric strain increments for equal pressure cycles (1.0 - 1.5 kg/cm²) on vertical and horizontal specimens. There was no need to recalculate them.

Mitchell's test results on kaolin will be employed to identify the basic material constants and the model parameters. For this purpose however, it is necessary to use a representative one-dimensional consolidation curve for kaolin. Such a curve has been plotted for the same saturated clay by Burland and Roscoe (1969) in which equilibrium average void ratios are plotted against the applied vertical effective pressures in a logarithmic scale, Figure (7).

The initial void ratio, e_0 , is estimated to be 4.18 using the elementary soil mechanics formula of $e_0 = G_s w$, with the specific gravity 2.61, and the initial water content $w = 1.6$

whereas the final value of void ratio at the end of one-dimensional consolidation at $\sigma'_{vc} = 2.5 \text{ kg/cm}^2 = 35.5 \text{ psi}$, can be obtained from Figure (7) as $e = 1.76$. The volumetric strain which is equal to the vertical strain in this case, corresponding to the maximum consolidation pressure and equal to μ_{11}^0 in the model is given by the equation

$$\mu_{11}^0 = \frac{e - e_0}{1 + e_0} \quad (26)$$

and is found to be 0.467. Although this value corresponds to the total strain, it may as well be assumed as equal to irrecoverable strain, since the unloading curve in Figure (7) is almost horizontal.

The values of the constants κ and C_p or C_{pl} are determined from the isotropic test. For isotropic conditions, elastic strain in equations (7) and (8) can be calculated for the two cases as

i) linear coupling:

$$\epsilon_{ij}^e = \frac{1}{3} \frac{\kappa}{1 + e_0} \ln (P'/P'_0) \delta_{ij} + C_p \mu_{ij} \mu_{kl} (\sigma'_{kl} - \sigma_{kl}^0) \quad (27)$$

ii) logarithmic coupling:

$$\epsilon_{ij}^e = \frac{1}{3} \frac{\kappa}{1 + e_0} \ln (P'/P'_0) \delta_{ij} + C_{pl} \mu_{ij} \ln \left(\frac{\mu_{kl} \sigma'_{kl}}{\mu_{kl} \sigma_{kl}^0} \right) \quad (28)$$

where $\mu_{11} \neq 0$ and $\mu_{22} = \mu_{33} \neq 0$.

Using the isotropic reloading curve from Figure (6) with the isotropic stress increment from 1.0 to 1.5 kg/cm^2 for the vertically trimmed specimen, together with equations (27) and (28), two equations can be written in each case for vertical and lateral elastic incremental strains. The values of the strain increments were taken as $d\epsilon_{11}^e = 0.43 \%$ and $d\epsilon_{33}^e = 0.05 \%$. It must be noted that in these equations, additional plastic strains accumulated during the stress cycle are added in the plastic prestrain μ_{ij} to the

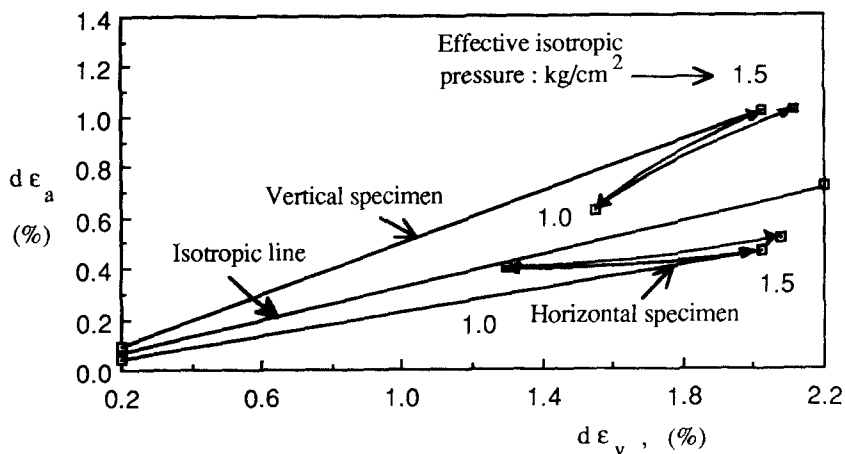


Figure 6: Incremental Volumetric Strains for Equal Pressure Cycles (1.0-1.5 kg/cm^2) on Vertical and Horizontal Specimens (after Mitchell, 1972)



Figure 7: One-Dimensional Consolidation Curve for Kaolin (after Burland and Roscoe, 1969)

preconsolidation strain μ_{11}^0 . Solving these equations simultaneously, the constant κ is found to be 0.0177. C_p and C_{pl} are found to be 3.362×10^{-2} for linear coupling and 1.851×10^{-2} for logarithmic coupling cases, respectively.

It must be noted that in the axial symmetry conditions for uniaxially or isotropically loaded specimens, the coincidence of principal axes of stress and strain is enforced.

The shear modulus G is obtained from the undrained triaxial compression tests. For triaxial conditions, equations (7) and (8) can be used together with Figure (4a) where the initial axial strain response of the vertical specimen in undrained test is plotted against the deviatoric stress. Writing these equations for the axial elastic strain, the shear modulus G is obtained as 257 kg/cm^2 or 25 MPa .

The configuration of the yield surface will now be established. At the end of anisotropic consolidation with $\sigma'_{vc} = 2.5 \text{ kg/cm}^2$, the yield surface has experienced a combined growth and rotation toward the K_0 line. Because $q/p = (q/p)_0$, no plastic demise mechanism is active at this stage, and $D = 0$ in equation (12). It may be seen using eq. (12) that the in situ yield surface is exactly centered on K_0 line. Employing the modified Jaky's equation for clays of $K_0 = 0.95 - \sin \phi'$, K_0 is found to be 0.575 for $\phi' = 22$ degrees, the latter value taken from Mitchell's tests. Hence, the lateral effective stress, σ'_h , at the end of consolidation can be estimated as 1.44 kg/cm^2 . These values for vertical and lateral effective stresses correspond to a mean isotropic effective stress of $p' = 1.79 \text{ kg/cm}^2$ and a deviatoric stress of $q = 1.06 \text{ kg/cm}^2$. Then, at K_0 condition, the angle θ is defined by an integrated form of (12), as $\theta = \theta_0 = \arctan (q / p')_0$ where $(q / p')_0 = 0.592$ which gives $\theta_0 = 30.63$. Note that at the end of consolidation the plastic deviatoric strain $\epsilon_q^p = (2/3) \epsilon_{11}^p = 0.3082$. The rotation of the yield surface due to shear is assumed to have been completed. Moreover, as explained below, the ratio q/p' during consolidation is maintained constant by assumptions related to the plastic potential. Figure (8) shows the rotated yield surface for which $a = 1.04 \text{ kg/cm}^2$ and $b = Na = 0.498 \text{ kg/cm}^2$ were determined. Note

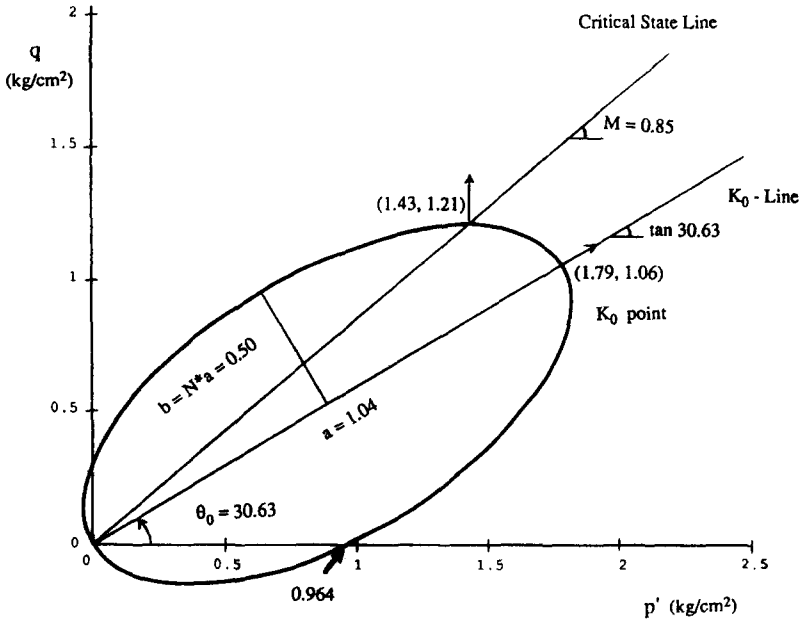


Figure 8: Predicted Yield Surface After Initial One-Dimensional Consolidation

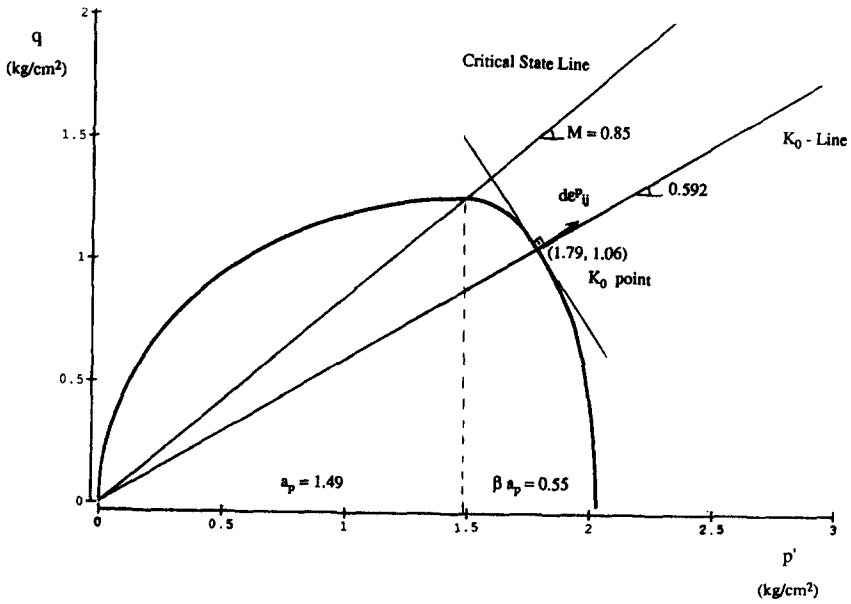


Figure 9: Predicted Plastic Potential After Initial One-Dimensional Consolidation

that, the assumption $dq/dp' = 0$ at the failure line $q/p' = M = 0.85$ was used to determine N .

To obtain the plastic potential, the following hypotheses are made. Since lateral plastic deformation is restrained during one-dimensional consolidation as discussed in the previous section, the vector of plastic strain rate is oriented in the direction of the vertical stress axis. Also, according to eq. (13), plastic strain rate is perpendicular to the plastic potential. Hence, at $\sigma'_v = \sigma'_{vc}$, along the potential

$$d\sigma'_v = dp' + \frac{2}{3} dq = 0 \quad (29)$$

which implies that the slope of plastic potential at K_0 point in q - p' plane is $-3/2$. Using this result with the known coordinates of K_0 point, the coefficient β was obtained as 0.37. The major semi-axis, a_p , of the plastic potential was found to be 1.49 kg/cm^2 . Plastic potential composed of two ellipses corresponding to the K_0 stress point (1.06, 1.79) is shown in Figure (9). Due to homothetic evolution of the potential during K_0 consolidation process governed by the requirement $d\varepsilon_{33}^p = d\varepsilon_{22}^p = 0$, a constant ratio q/p' is automatically maintained.

The last two constants, λ' being the slope of the isotropic consolidation curve, and γ being the constant of demise rate can be evaluated by the method of trials and errors from the isotropic incremental stress cycle of 1.0 to 1.5 kg/cm^2 , Figure (6). For the vertical specimen the initial stress for the isotropic loading $p' = 1.0 \text{ kg/cm}^2$, is almost exactly at the intersection of the p' axis with the rotated yield surface in Figure (8). Thus, the entire increment of volumetric plastic strain of 1.55 % is attributed to the stress increment of $dp' = 0.5 \text{ kg/cm}^2$, Figure (6). Note that, the shear contribution to the rotation equation (12) ceased at this stage, because of $q/p' = 0$. Thus, the rotation is now governed by the demise component (eq. 16) only. Hence, substituting for the

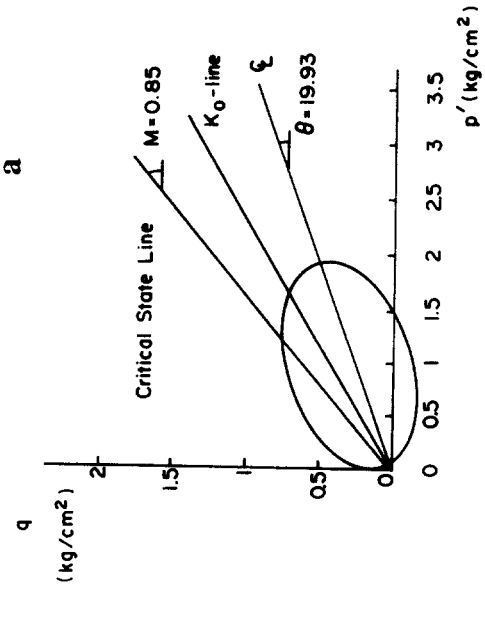


Figure 10: Predicted yield surface in different stages of the isotropic loading

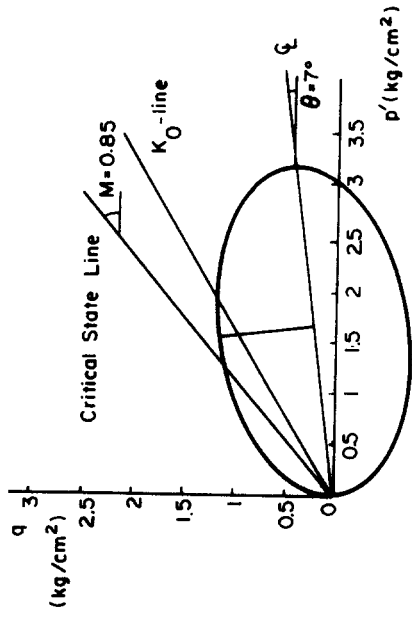


Figure 11: Predicted final position of the yield surface at the isotropic stress of 3 kg/cm²

multiplier $d\lambda$ in equation (24), the hardening modulus H through the hardening rules (11) and (16), the constants λ' and γ are numerically obtained. The values $\lambda' = 0.423$ and $\gamma = 25$ were found. The final configuration of the rotated yield surface at the end of this step is shown in Figure (10a). The angle of rotation at 1.5 kg/cm^2 decreased to 19 degrees.

NUMERICAL SIMULATION OF THE ISOTROPIC STRESS PATHS

In this section, the model prediction will be compared to Mitchell's data for isotropic stress path at higher stress level. In particular, the isotropic incremental stress cycle from 2.5 to 3.0 kg/cm^2 is investigated. The vectors OC_v , C_vD_v and OC_h , C_hD_h in Figure (5) represent the normalized strain increments developed in the vertical and horizontal specimens during this isotropic pressure cycle of 2.5 to 3.0 kg/cm^2 . The incremental strain values are normalized in this plot with respect to the maximum incremental axial strain.

Before simulating the material response for the above mentioned stress cycle, the yield surface has to be loaded isotropically up to the isotropic effective pressure of $p' = 2.5 \text{ kg/cm}^2$. This was achieved numerically with the value of volumetric plastic strain increment obtained as 0.044 for isotropic loading from 0.964 to 2.5 kg/cm^2 . It is of importance to note that the yield surface axis at $p' = 2.5 \text{ kg/cm}^2$ is now rotated only 10 degrees. The corresponding major axis, $2a$, of the yield surface at $p' = 2.5 \text{ kg/cm}^2$ has been calculated to be 2.8 kg/cm^2 . The new configuration of the yield surface due to isotropic loading to 2.5 kg/cm^2 is shown in Figure (10b).

During isotropic loading to $p' = 2.5 \text{ kg/cm}^2$, theoretically an equal plastic strain is accumulated in both the vertical and horizontal direction because of the assumed plastic potential evolution. The value of strain increment in each direction is found to be

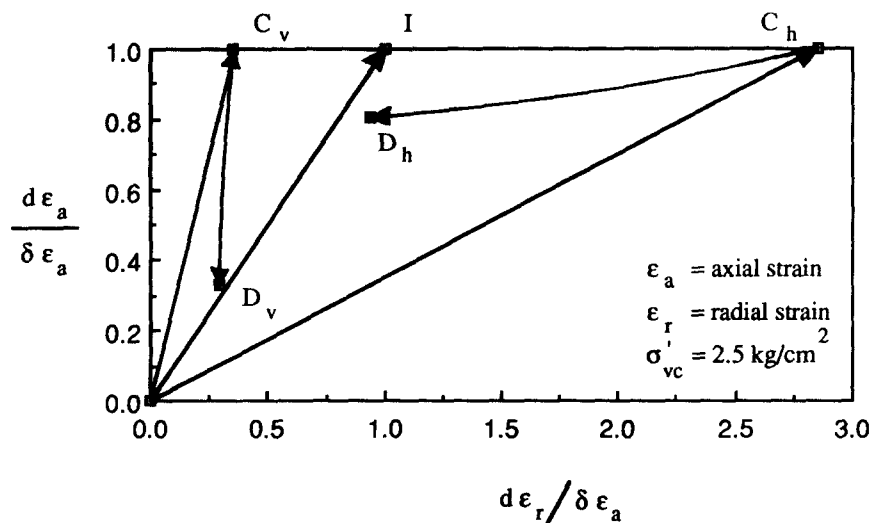


Figure 12: Calculated Strain Increment Response Using the Model with Linear Coupling, for $p' = 2.5$ to 3.0 kg/cm^2 Cycle

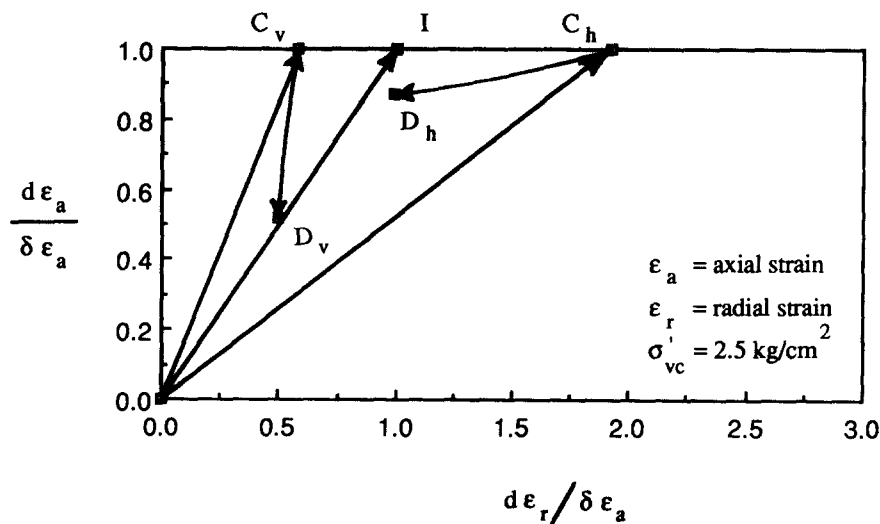


Figure 13: Calculated Strain Increment Response Using the Model with Logarithmic Coupling, for 2.5 to 3.0 kg/cm^2 Cycle

0.0149 which implies that the total value of the plastic prestrain in vertical direction has become $\mu_{11} = \mu_{11}^0 + \epsilon_{11}^p = 0.467 + 0.0149 = 0.482$ and the corresponding value in horizontal direction is $\mu_{33} = \epsilon_{33}^p = 0.0149$. Equations (21) and (22) specialized for the isotropic loading case, are used to calculate total strains. The new plastic potential corresponding to $p' = 2.5 \text{ kg/cm}^2$ and $q = 0$, is defined by a major semi-axis, a_p , of 1.83 kg/cm^2 .

To obtain numerical values of the total incremental strain accumulated during the isotropic stress cycle of 2.5 to 3.0 kg/cm^2 , equations (21) and (22) of the model for linear and logarithmic coupling respectively are used. Elastoplastic axial and radial strain increments calculated from these equations are plotted for both vertical and horizontal specimens in Figures (12) and (13). Note that the axial strain for vertical specimens is along the vertical deposit axis, whereas for horizontal specimens the axis of the specimen is oriented along one of the horizontal axes of the deposit, see again inset in Fig. (5). These incremental strains are normalized with respect to the maximum values of the axial strains to be able to compare to Mitchell's data. When compared to recalculated Mitchell's experimental results, the strain increment responses of Figures (12) and (13) should correspond to the strain increment response of Figure (5) represented by the vectors OC_v , C_vD_v and OC_h , C_hD_h . Figure (11) shows the configuration of the yield surface at 3.0 kg/cm^2 . It is seen that the rotation of the axis was diminished to 7 degrees. Thus almost all the anisotropy of the yield surface has been annihilated during the isotropic loading. This regress of anisotropy corresponds very well to observation of the undrained stress paths done by Mitchell, in Figure (4b). Considering only stress paths for the vertical specimen, it may be seen that the stress paths at 2.2 kg/cm^2 show yielding at a much higher value of the deviatoric stress, when compared to the stress path at 2.6 kg/cm^2 . In fact, the yield surface ellipse for 2.6 kg/cm^2 is expected to be less rotated than that at 2.2 kg/cm^2 , and consequently a vertical stress path across the surface will be shorter for 2.6 kg/cm^2 .

DISCUSSION AND CONCLUSIONS

It should be noted first that in both linear and logarithmic coupling case, the main feature of the anisotropy, highlighted by the Mitchell's results, namely, the presence of deviatoric strain in isotropic loading is well reproduced in the simulation. The deviation from isotropy is manifested by the departure of the strain vector OC_v and OC_h from the isotropic line OI in Figs 5., 12 and 13. The logarithmic coupling gives a better approximation. The linear coupling overestimates the elastic part of strain, both in vertical and horizontal specimens. For the horizontal specimen the simulation of logarithmic coupling is in nearly perfect agreement with experiment (see OC_h and C_hD_h in Fig. 5). Clearly, the coupling strain rate part, which in linear law is assumed as proportional to stress rate, grows too much, while in the logarithmic law it is normalized with respect to the value of isotropic stress and its growth is more moderate. Thus, it is concluded from the simulation results that in lightly overconsolidated kaolin, logarithmic coupling is more realistic than the linear coupling.

Furthermore, Figure (14) shows the values of the total incremental strain components predicted by the model using the logarithmic approach for the isotropic loading from 1.0 to 3.0 kg/cm² for vertical specimens. It is observed that the values of horizontal strains are much lower than the vertical ones. This indicates now the anisotropic behavior of the soil upon isotropic loading influenced by the initial one-dimensional consolidation. No comparison with Mitchell's data was possible because of lack of experimental data on the loading step from 1.5 to 2.5 kg/cm². Figure (15) illustrates the calculated relative amounts of the incremental strains for both isotropic loading cycles predicted by the simulation with logarithmic approach. It must be noted that as the isotropic pressure increases, even with the same amount of incremental isotropic pressure of 0.5 kg/cm², the values of incremental strains decrease as should be expected.

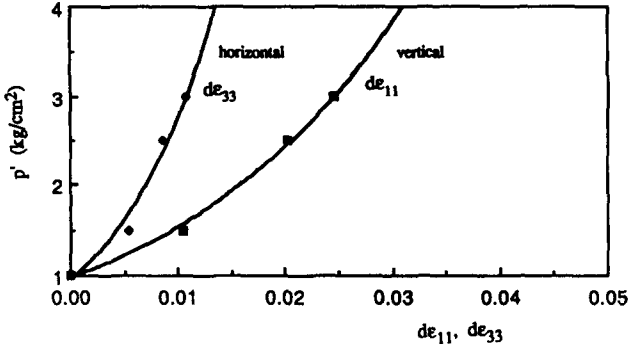


Figure 14: Total Strain Components Predicted for the Isotropic Loading from 1.0 to 3.0 kg/cm² for Vertical Specimen Using Logarithmic Coupling Approach

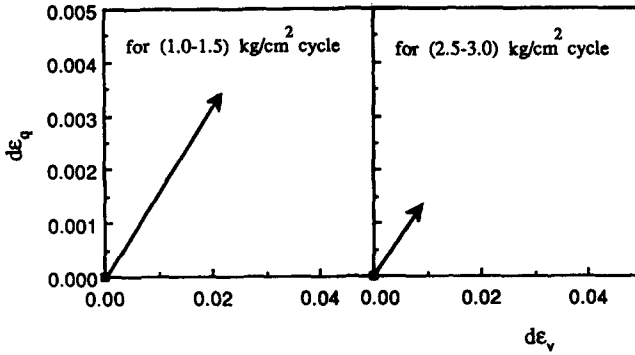


Figure 15: Total Incremental Strains for the both Isotropic Loading Cycles Predicted by the Simulation with Logarithmic Coupling Approach

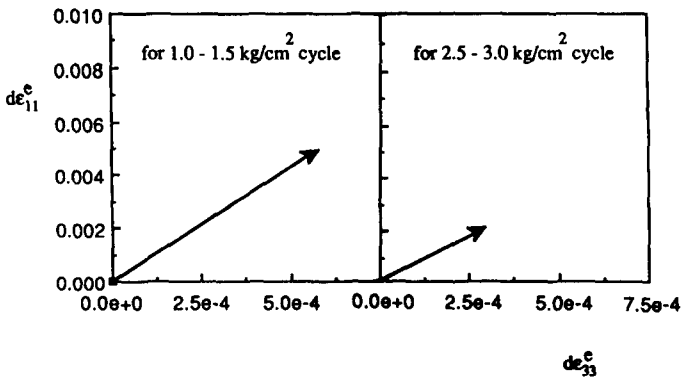


Figure 16: Elastic Incremental Strains for the both Isotropic Loading Cycles Predicted by the Simulation with Logarithmic Coupling Approach

It is of special interest to note that both in the simulation of the logarithmic case and in the experimental plots of Mitchell, elastic radial strains start to build up during the isotropic stress cycle of 2.5 to 3.0 kg/cm². This is not observed, however, before the isotropic pressure cycle of 1.0 to 1.5 kg/cm² starting at 1.0 kg/cm² which corresponds to the end of the initial one-dimensional consolidation. This effect is referred to as anisotropy demise and is illustrated in Figure (16) where the inclination of the elastic part of the strain rate components are shown for the two loading stages (1.0-1.5 kg/cm² and 2.5-3.0 kg/cm²). It is seen that the strain rate vector starts slowly to rotate as the isotropic load increases. The other effect of anisotropy demise, the regress of the rotation the yield surface during isotropic compression, is also simulated quite accurately. In fact, at 3.0 kg/cm² the rotation demise is almost completed, as it is in the experiments by Mitchell (1972). Thus, it appears that the rate of the plastic anisotropy demise is greater than that of elastic anisotropy.

ACKNOWLEDGMENTS

The support by a contract from ISMES Spa., Bergamo, Italy, is gratefully acknowledged.

REFERENCES

- Amarasinghe, S.F., and Parry, R.H., (1975), "Anisotropy in Heavily Overconsolidated Kaolin", *Journal of Geotechnical Engineering Division, ASCE*, Vol. 101, No. GT12, 1975, pp. 1277-1292.
- Anandarajah, A., and Dafalias, Y.F., (1986), "Bounding Surface Plasticity, III: Application To Anisotropic Cohesive Soils", *Journal of Engineering Mechanics, ASCE*, Vol. 112, No. 12, Dec. 1986, pp. 1292-1318.
- Atkinson, J.H., (1975), "Anisotropic Elastic Deformations in Laboratory Tests on Undisturbed London Clay", *Geotechnique* 25, No. 2, pp. 357-374.
- Banerjee, P.K., Stipho, A.S., and Yousif, N.B., (1984), "A Theoretical and Experimental Investigation of the Behavior of Anisotropically Consolidated Clays", *Developments in Soil Mechanics and Foundation Engineering, Vol. II*, P.K. Banerjee and R. Butterfield, Eds., Elsevier Applied Science, London, U.K., 1984, pp. 1-41.
- Bennett, R.H., and Hulbert, M.H., (1986), *Clay Microstructure*, IHRDS, Boston, 1986.
- Burland, J.B., (1967), "The Deformation of Soft Clay", PhD. thesis, Cambridge University, 1967.
- Burland, J.B., and Roscoe, K.H., (1969), "Local Strains and Pore Pressures In a Normally Consolidated Clay During One-Dimensional Consolidation", *Geotechnique* 19, No. 3, pp. 335-356.
- Dafalias, Y.F., (1977), "Elastoplastic Coupling within a Thermodynamic Strain Space Formulation of Plasticity", *Int. Journal of Non-linear Sci.*, 12, pp. 327-337.
- Dafalias, Y.F., and Hermann, L.R., (1982), "Bounding Surface Formulation of Soil Plasticity", *Soil Mechanics - Transient and Cyclic Loads*, G.N. Pande and O.C. Zienkiewicz, Eds., John Wiley and Sons, Chichester, U.K., 1982, pp. 253-282.

- Drescher, A., Hueckel, T., and Mroz, Z., (1974), "Multiple and Reverse Shear Method of Testing Mechanical Properties of Powders", *Bulletin of Polish Acad. of Sciences*, 23, pp. 405-414.
- Graham, J., Noonan, M.L., and Lew, K.V., (1983), "Yield States and Stress-Strain Relationships In a Natural Plastic Clay", *Canadian Geotechnical Journal*, 20, pp. 502-516.
- Hashiguchi, K., (1979), "Constitutive Equations of Granular Media with an Anisotropic Hardening", *Proceed. of the Third Int. Conf. on Num. Methods in Geomechanics*, Aachen, W. Germany, April 2-6, 1979.
- Hirai, H., (1989), "A Combined Model for Anisotropically Consolidated Clays", *Soils and Foundations*, Japanese Society of Soil Mechanics and Foundation Engineering, Vol. 29, No. 3, September, 1989, pp. 14-24.
- Hueckel, T., and Drescher, A., (1975), "On Dilational Effects of Inelastic Granular Media", *Archivum Mechaniki Stosowanej*, 27, 1, Warsaw.
- Hueckel, T., (1976), "Coupling of Elastic and Plastic Deformation of Bulk Solids", *Meccanica*, 11, 1976, pp. 227-235.
- Hueckel, T., (1985), "Discretized Kinematic Hardening in Cyclic Degradation of Rocks and Soils", *Engineering Fracture Mechanics*, 21, 4, pp. 923-945.
- Jaky, J., (1944), "A Nyugalmi nyomas tenyezoje", *Magyar Mernok es Epitesz Kozlonye*, pp. 355-358.
- Jamiolkowski, M., Ladd, C.C., Germaine, J.T., and Lancelotta, R., (1985), "New Developments in Field and Laboratory Testing of Soils", *State of the Art Report, XI ICSMFE*, San Francisco, 1985, A. A. Balkema.
- Kavvas, M.J., (1983), "A Constitutive Model for Clays Based on Non-associated Anisotropic Elasto-plasticity", *Proceed. of the Int. Conf. on Constitutive Laws for Engineering Materials - Theory and Application*, Tucson, Arizona, Jan. 10-14, 1983, pp. 263-270.

- Ko, H. Y. and Sture S. (1980), *Data Reduction for Analytical Modelling, State of the Art Paper*, Pres. ASTM Symposium, Chicago, Ill.
- Lambe, T.W., and Whitman, R.V., (1979), *Soil Mechanics*, John Wiley and Sons., 1979.
- Lewin, P.I., and Burland, J.B., (1970), "Stress Probe Experiments on Saturated Normally Consolidated Clay", *Geotechnique* 20, 1, pp. 38-56.
- Mitchell, R.J., (1972), "Some Deviations from Isotropy in a Lightly Overconsolidated Clay", *Geotechnique*, 22, 3, 459-467.
- Murff, J.D., (1982), Private Communications, (see Abaqus, User Manual, 1990).
- Ohta, H., and Sekiguchi, H., (1979), "Constitutive Equations Considering Anisotropy and Stress Reorientation in Clay", *Third Int. Conf. on Num. Met. in Geomechanics*, Aachen, 1979, pp. 475-484.
- Prager, W., (1956), "A New Method of Analyzing Stress and Strain in Work-Hardening Plastic Solids", *J. Appl. Mechanics*, 23, page 493.
- Prevost, J.H., (1978), "Plasticity Theory for Soils' Stress-Strain Behavior", *Journal of the Engineering Mechanics Division, ASCE*, Vol. 104, No. EM5, Oct., 1978, pp. 1177-1196.
- Roscoe, K.H., and Burland, J.B., (1969), "On the Generalized Stress-Strain Behavior of Wet Clays", *Engineering Plasticity*, J. Heyman and F.A. Leckie, Eds., Cambridge University Press, 1969, pp. 535-609.
- Schofield, A.N., and Wroth, C.P., (1968), *Critical State Soil Mechanics*, McGraw - Hill, 1968.
- Tavenas, F., and Leroueil, S., (1977), "Effects of Stresses and Time on Yielding of Clays", *Proceed. of the IX Int. Conf. on Soil Mechanics and Foundation Engineering*, Vol. 1, Tokyo, Japan, 1977.
- Ziegler, H., (1959), "A Modification of Prager's Hardening Rule", *Quarterly of Applied Mathematics*, 17, pp. 55-65.

APPENDIX I

A general 3-dimensional representation of the yield surface can be achieved considering an ellipsoid in the principal stress space, centered in the direction of a radius crossing the origin. The ellipsoid equation is expressed in a $q - p' - r$ coordinate system, where p' is the hydrostatic axis along $\sigma_1' = \sigma_2' = \sigma_3'$; q is the axis normal to it and belonging to so called triaxial plane ($\sigma_2' = \sigma_3'$); finally r is the axis whose unit vector is perpendicular to the usual triaxial $q - p'$ plane and oriented according to give the left handed Cartesian system q, p' and r . Figure (A1.1) shows such a yield surface in the form of an ellipsoid centered along a known radius line in $q - p' - r$ stress space. The rotation in $q - p'$ plane depends on plastic deviatoric strain component and is defined by the angle of rotation θ . In order to orient the apex of the ellipsoid along a line off the triaxial plane, an additional angle of rotation around q axis is required. Hence, α being this additional rotation angle, the equation (9) of the yield function can be rewritten in 3-dimensional stress space as follows

$$\left[\frac{(p' + q \tan \theta - r \tan \alpha / \cos \theta)}{a / (\cos \theta \cos \alpha)} - 1 \right]^2 + \left[\frac{(p' \tan \alpha + q \tan \theta \tan \alpha + r / \cos \theta)}{N a / (\cos \theta \cos \alpha)} \right]^2 + \left[\frac{(-p' \tan \theta + q)}{N a / \cos \theta} \right]^2 - 1 = 0 \quad (\text{A1.1})$$

The angle θ and α are functions of the plastic strain. In particular, the rotated yield surface is assumed to correspond to the initial anisotropy achieved during pre-consolidation. At the end of the pre-consolidation, the major semi-axis of the yield surface is directed along the radius defined by the maximum pre-consolidation stress. In the case of transverse isotropy, in one dimensional K_0 consolidation, where $\sigma_2' = \sigma_3'$, $\alpha = 0$. The hardening equation governing the additional rotation angle α of the yield surface around q axis, is

assumed to depend on the third invariant of deviatoric plastic strain and can be expressed through a non-linear rate evolution equation

$$d(\tan \alpha) = \frac{r}{p'} [\eta \exp(-\eta \epsilon_r^p)] d\epsilon_r^p \quad (\text{A1.1})$$

where $\epsilon_r^p = \left(\frac{1}{3} \epsilon_{ik}^p \epsilon_{jk}^p \epsilon_{ij}^p\right)^{\frac{1}{3}}$, η is a model parameter similar to δ . During an advanced consolidation stage, exponential term tends to zero and the rate of $\tan \alpha$ tends to the current value of r/p' .

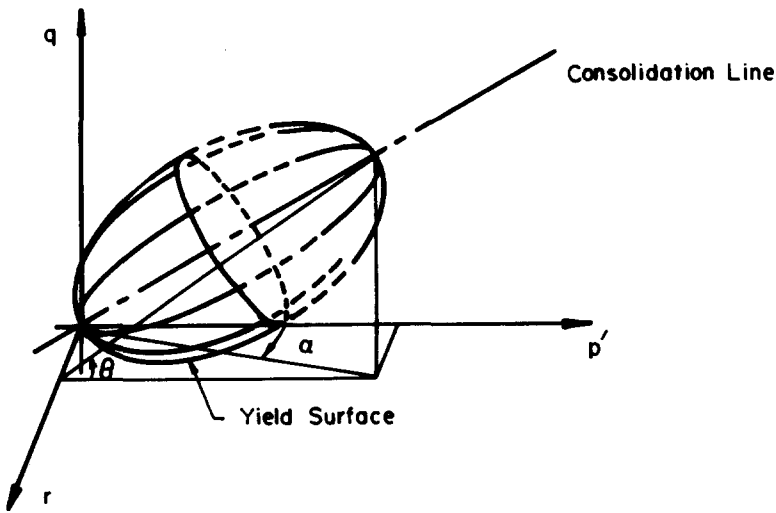


Figure A1: Representation of the rotated yield surface in an invariant space

APPENDIX II

Of special interest is a simplified formulation for the triaxial apparatus conditions, with an additional assumption that only inherent anisotropy is taken into account. The latter assumption implies that the only non-zero component of μ_{ij} is $\mu_{11} = \mu_{11}^0 = (\epsilon_{11}^p)$ at K_0 , which is plastic vertical strain accumulated during the uniaxial pre-consolidation. Consequently, the material becomes transversely isotropic.

i) linear coupling:

$$d\epsilon_v = \left\{ \frac{\kappa}{1 + e_0} \frac{dp'}{p'} + C_p (\mu_{11}^0)^2 d\sigma'_{11} \right\} + d\lambda \left\{ C_p \left[\Delta\sigma'_{11} \mu_{11}^0 \frac{\partial g}{\partial p'} + \Delta\sigma'_{kl} \mu_{11}^0 \frac{\partial g}{\partial \sigma'_{kl}} \right] + \frac{\partial g}{\partial p'} \right\} \quad (A2.1)$$

$$d\epsilon_q = \frac{1}{2G} dq + \frac{2}{3} C_p (\mu_{11}^0) \frac{d\sigma'_{11}}{\sigma'_{11}} + d\lambda \left\{ C_p \left[\Delta\sigma'_{11} \mu_{11}^0 \frac{\partial g}{\partial q} + \frac{2}{3} \Delta\sigma'_{kl} \mu_{11}^0 \frac{\partial g}{\partial \sigma'_{kl}} \right] + \frac{\partial g}{\partial q} \right\} \quad (A2.2)$$

where $\Delta\sigma'_{kl} = \sigma'_{kl} - \sigma'^0_{kl}$.

ii) logarithmic coupling:

$$d\varepsilon_v = \left\{ \frac{\kappa}{1 + e_0} \frac{dp'}{p'} + C_{pl} \mu_{11}^0 \frac{d\sigma'_{11}}{\sigma'_{11}} \right\} + d\lambda \left\{ C_{pl} \left[\ln \left(\frac{\mu_{11}^0 \sigma'_{11}}{M_{10}} \right) \right] \frac{\partial g}{\partial p'} + \frac{\sigma'_{kl}}{\sigma'_{11}} \frac{\partial g}{\partial \sigma'_{kl}} \right] + \frac{\partial g}{\partial p'} \right\} \quad (\text{A2.3})$$

$$d\varepsilon_q = \left\{ \frac{1}{2G} dq + \frac{2}{3} C_{pl} \mu_{11}^0 \frac{d\sigma'_{11}}{\sigma'_{11}} \right\} + d\lambda \left\{ C_{pl} \left[\ln \left(\frac{\mu_{11}^0 \sigma'_{11}}{M_{10}} \right) \right] \frac{\partial g}{\partial q} + \frac{2\sigma'_{kl}}{3\sigma'_{11}} \frac{\partial g}{\partial \sigma'_{kl}} \right] + \frac{\partial g}{\partial q} \right\} \quad (\text{A2.4})$$

Received 7 May 1993; revised version received 25 August 1993; accepted 27 August 1993